ANALYSIS FOR HETEROGENEOUS BLANKETS AND COMPARISON TO MEASUREMENTS: PHASE IIC EXPERIMENTS OF THE USDOE/JAERI COLLABORATIVE PROGRAM ON FUSION NEUTRONICS

M. Z. Youssef, A. Kumar, M. Abdou
Mechanical, Aerospace and Nuclear Engineering
University of California at Los Angeles
Los Angeles, CA 90024, U.S.A.
(213) 825-2879

M. Nakagawa, K. Kosako, Y. Oyama, and T. Nakamura
Japan Atomic Energy Research Institute
Tokai-mura, Naka-gan, Ibaraki-ken, 319-11
011-81-(292) 82-6016

ABSTRACT

Effort in Phase IIC of the US/JAERI Collaborative Program on Fusion Neutronics was focused on performing integral experiments and post analyses on blankets that include the actual hetergeneities found in several blanket designs. Two geometrical arrangements were considered, namely multi-layers of Li_2O and beryllium in an edge-on, horizontally alternating configuration for a front depth of 30 cm, followed by the Li_2O breeding zone (Be edge-on, BEO, experiment), and vertical water coolant channels arrangement in which one is placed behind the first wall and two other channels (width of 0.5 cm each) are placed at depths of 10 and 30 cm from the first wall (WCC experiment). The objectives are to experimentally verify the enhancement in tritium production in the first experiment and to examine the accuracy of predicting tritium production and other reaction rates around these heterogeneities in the two experiments. In the BOE system, it was shown that, with the zonal method to measure tritium production from natural lithium (Tn), the calculated-to-measured values (C/E) are 0.95 - 1.05 (JAERI) and 0.98 - 0.9 (U.S.), which is consistent with the results obtained in other Phases of the Program. In the WCC experiment, there is a noticeable change in C/E values for T_6 near the coolant channels where steep gradients in T_6 production are observed. The C/E values obtained with the Li-foils to measure T_6 are better than those obtained by the Li-glass method. As for T_7, calculations and measurements by NE213 method are within ± 15% in JAERI's analysis, but larger values (~ 20-25%) are obtained in the U.S. analysis. Around heterogeneities, the prediction accuracy for T_7 is better than that for T_6. In both experiments, the prediction accuracy for high-threshold reactions [(e.g. $^{93}Nb(n,2n)$] is within ± 10% as obtained by both Monte Carlo and Sn codes, however, it was shown that the $^{58}Ni(n,2n)$ cross-section of ENDF/B-V should be increased by 25-30% at high incident neutron energies to give better C/E values.

INTRODUCTION

Conceptual blanket design for fusion reactors includes a heterogeneous arrangement of more than one material that serves a particular function for efficient energy extraction. For solid breeder blankets, the inclusion of coolant and purge gas channels in the design causes considerable distortion in the neutron energy spectrum around these heterogeneities with a consequent impact on local tritium production and heating rates at these locations. In addition, the utilization of materials that have different neutronic characteristics (e.g. first wall, multiplier, breeding material, etc.) also introduces local, and in some cases, sharp variation in the neutron spectrum at the interfaces of these materials. Often, designers follow a homogenization procedure in their calculational models, particularly when the blanket includes complex features of multi-components, in order to simplify the models used to predict the nuclear performance of the blanket and this naturally leads to large uncertainties in the prediction of local effects and perhaps global quantities such as tritium breeding in a fusion blanket.

Two fusion-oriented integral experiments that focused on these heterogeneous effects were performed at the Fusion Neutronics Source (FNS) facility at Japan Atomic Energy Research Institute (JAERI) during the fall of 1988 and marked the completion of Phase IIC of the On-going USDOE/JAERI Collaborative Program on Fusion Neutronics. Phase I, Phase IIA and IIB experiments of this program were completed and the progress achieved during these phases were reported and/or published elsewhere (refs. 1-11). During these phases, several integral experiments were performed utilizing a 14 MeV point source and proceeded from a simple one-material (Li_2O) test assembly to a more prototypical one that includes the engineering features of a fusion blanket, e.g., First wall, multiplier, and coolant channels. Emphases were placed in phase IIA on studying the impact of using beryllium as a multiplier in different configurations (e.g. as a front layer or sandwiched between two Li_2O layers) on the neutronic characteristics of the Li_2O test assembly, and in particular, on the tritium production profiles both locally and in central zones throughout the test assembly .[4-11] Phase IIB configuration is similar to that of Phase IIA, except that beryllium was used as an inner liner[10-11] and thus acts as an armor material normally utilized on the inboard of a Tokamak reactor. Unlike the earlier Phase I experiments in which an open geometry was used[1-3], in Phase IIA, IIB, and IIC (the subject of this paper), the incident neutron spectrum on the test assembly closely simulates the incident neutron spectrum that is found in fusion reactors and that is due to the careful selection of materials [e.g., Li_2CO_3, polyethylene (PE)] and configuration for these phases of the experiments.

In all these experiments, the prediction accuracies by using various codes and data libraries for key neutronics parameters, such as tritium production rate (TPR) from ^6L_i (T_6) and ^7L_i (T_7), are checked against the measured ones to arrive at estimates for the experimental and analytical uncertainties associated with these parameters. Tritium production rate (both locally and inside zones) is the prime focus in these phases with an attempt to extrapolate the estimated uncertainties to reactor conditions. This latter goal will be better achieved upon the completion of Phase III experiments started during the fall of 1989 in which a line source was simulated by the movement of the annular blanket back and forth relative to the stationary 14 MeV point source.[14-17] The prediction accuracy for other parameters of importance for blanket designers such as nuclear heating and decay heat will also be emphasized in Phase III of this Collaborative Program.[18]

In Section II, the experiments performed on heterogeneous effects in Phase IIC for which the analysis is given in this paper are briefly described. More detailed experimental data for these experiments can be found in a companion paper (Ref. 12). The calculational methods followed in analyzing these experiments are described in Section III, while the analytical results and comparison to the experimental data are given in section IV. Section V summarizes the main findings in this study along with recommendations for blanket designers.

II. THE EXPERIMENTS

The test assembly (Li_2O), for which the prediction accuracies for heterogeneous effects are examined, is placed at one end of a rectangular Li_2CO_3 enclosure of a 20 cm thickness which is isolated from the surroundings by a 5 cm thick polyethylene (PE) layer (See Fig. 1, Ref. 7). This layer minimizes the neutron room-returned component that reach the test assembly. A water-cooled rotating neutron target (RNT) is used to generate the intense 14 MeV neutron source and is located in the inner cavity. The outer dimensions of the rectangular Li_2CO_3 assembly is ~ 136 cm x 136 cm x 235 cm and is made of sintered blocks of various sizes. The two experiments considered are:

(a) The Water Coolant Channel (WCC) arrangement: In this experiment the water channels consisted of 5 mm thick polyethylene (to simulate water coolant) structured between two layers of S.S., each 0.7 mm thick. One coolant channel was placed behind a 5 mm thick SS FW and preceded the Li_2O test assembly (of thickness ~ 60 cm). Two other coolant channels were placed at a depth of 10 cm, and 20 cm, respectively, from the front surface of the assembly as shown in Fig. 1. This figure shows the geometrical details of the test assembly itself that is housed at one end of the Li_2CO_3 enclosure. The front rectangular surface of the test assembly has dimensions of 86.2 cm x 86.2 cm A radial drawer was also installed horizontally, as shown in Fig. 1. These drawers have a cross-sectional area of 5.06 cm x 5.06 cm and they extend throughout the Li_2O assembly and the Li_2CO_3/PE layers.

(b) The multi-layered Beryllium Edge-On arrangement (BEO): In this experiment, multiple layers of Li_2O and beryllium were arranged in an edge-on, horizontally alternating configuration for a front depth of 30 cm followed by the Li_2O breeding zone (see Fig. 1). Two central drawers and one radial drawer (filled with Li_2O) were also installed in this experiment.

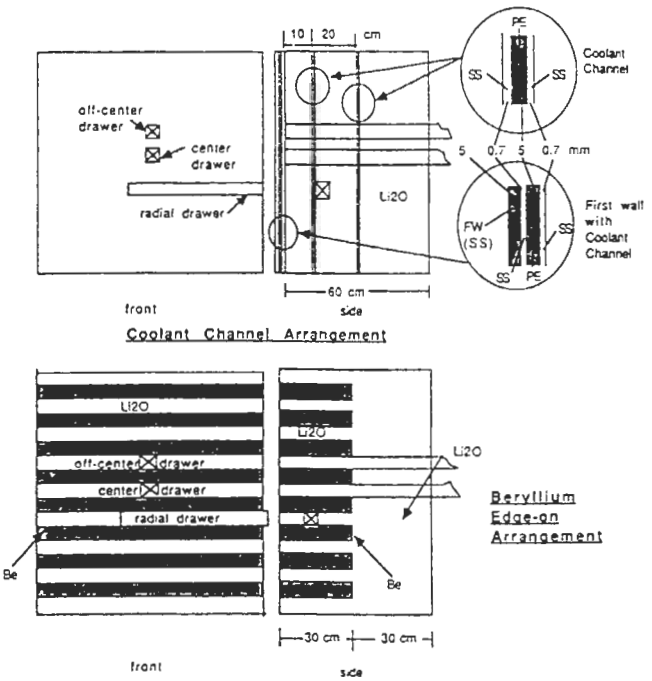

Figure 1. Configurations of the test assembly in the coolant channel and the Beryllium edge-on experiments.

The locations and the dimensions of the coolant channels in the WCC experiment have been chosen to be representative of channels found in a typical fusion blanket. The multi-layer arrangement of Be/Li_2O in the first 30 cm of the BEO experiment has also been chosen after extensive pre-analysis aimed at examining the optimal arrangement of equal volumes of beryllium and Li_2O in a front zone of thickness 20-30 cm that gives the largest tritium production rate. It was shown that the intermixing of horizontal Be and Li_2O layers in an edge-on arrangement is superior to the vertical arrangement of alternating Be and Li_2O layers as far as the TPR is concerned.[13] This is an important feature to be considered by blanket designers.

The TPR from $^6Li(T_6)$ was measured by Li-glass detectors along the central drawer in the WCC and BEO experiments. It was also measured by Li-foil detectors along the central drawer in the WCC experiment using ^7Li-enriched and Li-natural (^NLi) foils. In the BEO experiment, ^7Li-enriched foils were used in the central drawer while ^NLi foils were utilized in the off-central drawer to measure T_6 and T_7. The NE213 detectors were also used to measure T_7 along the central drawer in the WCC and BEO experiments by folding the measured spectrum with the response $^7Li(n,n'\alpha)t$ cross-section (indirect method). In addition to local TPR measurements, zonal tritium production rates were measured in pre-designated blocks along the central drawer (^7Li-enriched blocks) and the off-central drawer (^NLi-blocks) in the BEO system.

The in-system spectrum measurements were preformed by using small spherical NE213 detectors in the energy range $E_n > 1$ MeV and by using small size proton recoil counters (PRC, H_2 and H_2/Ar filled) in the energy range 1 KeV < E_n < 1 MeV. These measurements were taken along the central axis in the WCC experiment (NE213 measurements) and the BEO experiment (both NE213 and PRC measurements). Foil activation measurements along the off-central drawer in the WCC experiment were performed for the reactions $^{58}Ni(n,2n)$,$^{58}Ni(n,p)$,$^{93}Nb(n,2n)^{92m}Nb$,$^{115}In(n,n')^{115m}In$, $^{27}Al(n,\alpha)$, and $^{197}Au(n,\gamma)$. Except for the $^{197}Au(n,\gamma)$, these reactions have threshold energies (E_{th}) of ~ 13 MeV, ~ 2 MeV, ~ 10 MeV, ~ 0.5 MeV and ~ 6 MeV, respectively. Because of the difference in these threshold energies, comparison between measurements and calculations for these reactions provides useful information on the neutron spectrum inside the Li_2O assembly and complements the NE213 and proton recoil measurements. These reactions were also measured in the BEO system along the central drawer in addition to the $Ti(n,x)^{46}Sc$, $Ti(n,x)^{47}Sc$ and $Ti(n,x)^{48}Sc$ reactions. Because the $^{197}Au(n,\gamma)$ reaction occurs at all energies, this reaction was used to infer the degree of accuracy in predicting T_6 which has a substantial component at low energies. In the BEO system, vertical distribution of this reaction was measured at the front surface of the Be/Li_2O layers and at a depth of ~ 10 cm This mapping was made to indicate the variation in the low-energy component of the neutron flux as one moves alternatively between the Be and Li_2O layers. Details of the measurements performed in this phase can be found in Ref. 12.

III. CALCULATIONAL METHODS

In analyzing the WCC experiment, both deterministic and Monte Carlo methods were independently used by the U.S. and JAERI. Monte Carlo codes were used in analyzing the BEO experiment. The MCNP code (Version 3B) was used by the U.S. along with its point wise continuous energy/angle cross-section library RMCCS/BMCCS based on ENDF/B-V, version-2, data. The MORSE-DD code has been used by JAERI and it utilizes the double differential cross-section library DDL/J3P1 (125 neutron groups) based on JENDL3/PR1 data base. The codes used by the U.S. in the 2-D Sn method were DOT 5.1 in conjunction with the first collision code, RUFF.[22] It was necessary to use the RUFF code since it is compatible with DOT 5.1 when the variable mesh feature is used as is the case in the U.S. calculations. The DOT 5.1 is an advanced version of the DOT 4.3 code.[23] In JAERI's calculations, the DOT 3.5[24] and GRTUNCL[24] codes were used. In the 2-D calculations, the RUFF and GRTUNCL codes were necessary in order to mitigate the ray effects in the discrete ordinates codes when applied with an external point source. In the U.S. calculations, the P_5 - S_{16} approximation was adopted and the MATXS6 library (80-g) was used which was previously generated using the TRANSX-CTR processing code[25] and is based on ENDF/B-V (version 2). The FSXJP7 library (P_7, 125-g) was used in JAERI's calculations and is based on JENDL3/PR2.

The dimensions as adopted in the calculations for the two experiments are shown in Figure 2 (shown are the inner dimensions of the cavity and the test assembly). It was necessary to calculate the angular and energy distribution of the incident neutrons using the Monte Carlo method to account for the complex nature of the rotating neutron target. These calculations were previously discussed.[2-3] The calculational procedures and modeling are very similar to those used in Phase IIA and IIB and more details can be found in Refs. 4,6,8,10, and 11. For example, Fig. 3 shows the 2-D R-Z model used in the DOT 5.1 calculations for the WCC experiment where part of the target is shown. The energy and angular distribution of neutrons produced at the beam spot z = r = 0.0 has been calculated based on the formula of Benveniste et al.[26] and on the D-T kinematics of the corresponding D^+ beam energy. The atomic densities of materials used in the WCC experiment are given in Table 1.

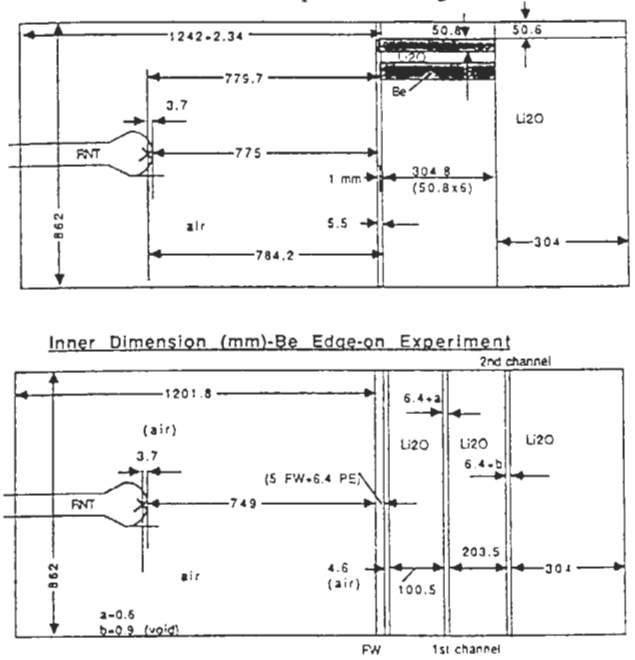

Figure 2. Inner dimensions (mm) of the inner cavity and test assembly in the coolant channel and Be edge-on experiments.

IV. ANALYTICAL RESULTS AND COMPARISON WITH EXPERIMENTAL VALUES

IV.A Coolant Channels Experiment (WCC)

The introduction of coolant channels behind the first wall and inside the Li_2O assembly tends to appreciably soften the neutron spectrum inside and around them due to neutron moderation by the coolant. Consequently, reactions that are sensitive to the low-energy component of the neutron spectrum are noticeably large around these heterogeneities. The pre-analysis[13] for the selection of the configuration for this experiment had indicated an increase in T_6 by as much as a factor of 2 - 3 in zones around coolant channels in comparison to the case where no channels are deployed. In the WCC experiment, theT_6 profiles are very steep at the boundaries of the Li_2/WCC with a local increase by a factor of 4 - 6. Since T_7 is only sensitive to the high-energy component of the neutron spectrum, these sudden changes in local values do not occur in the T_7 profile.

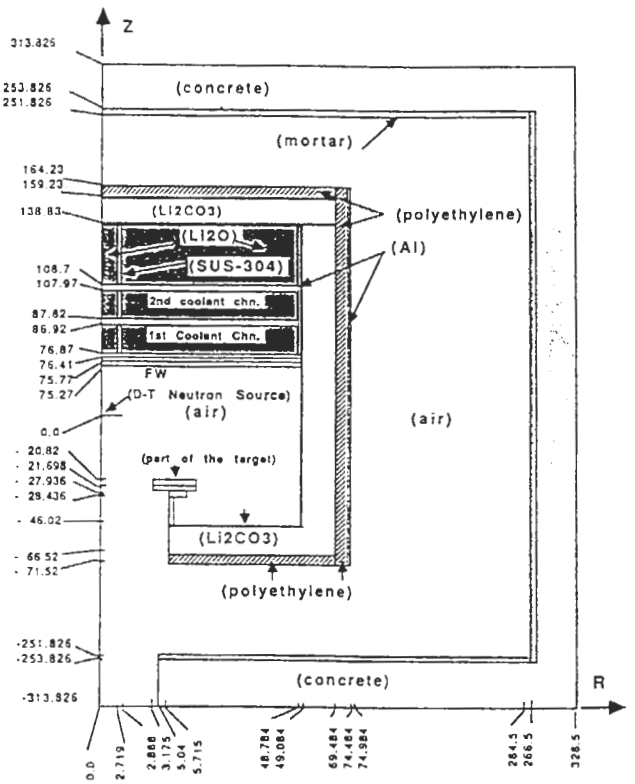

Figure 3. The 2D R-Z model of DOT 5.1 calculations (WCC Experiment).

Table I: Atomic Densities ($x10^{-24}$) of Materials Used in the 2D Calculational Model for the Coolant Channel Experiment(+)

Element	Inner Li_2O (Drawer)	Outer Li_2O	S.S. Between Inner and Outer Li_2O	FW	S.S. Coolant Channel
Fe	4.894-4*	1.092-3	2.514-2	6.022-2	5.987-2
Cr	1.358-4	3.027-4	6.976-3	1.683-2	1.514-2
Ni	5.937-5	1.325-4	3.050-3	7.426-3	8.389-3
Mn	1.086-5	2.422-5	5.577-4	8.440-4	9.945-4
			Li_2CO_3		
^6Li	4.250-3	4.215-3	1.719-3		
^7Li	5.314-2	5.270-2	2.425-2		
^{16}O	2.869-2	2.846-2	4.021-2		
	Concrete	Mortar			
H	7.976-3	3.768-2	5.631-4		
Na	7.859-4	5.080-4	8.928-4		
Ca	2.564-3	3.714-3	8.194-5		
Mg	3.824-4	4.687-4			
Si	1.481-2	1.135-2	8.186-5	7.632-4	3.432-4
Al	2.637-3	1.941-3			
K	5.288-4	3.343-4	8.193-4		
C	5.288-4	7.430-4	1.424-2	1.983-4	4.513-5
^{16}O	4.315-2	9.425-3			
Fe	5.859-4	6.810-4			

* Reads 4.894×10^{-4}
\+ PE (coolant channel) H: 8.257-2, C: 4.128-2
PE (outer layer) H: 8.146-2, C: 4.073-2

IV.A.1 In-System Neutron Spectrum

The neutron spectrum was measured at several locations along the axis of the central drawer using NE213 detectors. Figs. 4 shows a comparison of the calculations (JAERI: MORSE-DD and DOT 3.5; U.S.: MCNP and DOT 5.1) and measurements (NE213) at a depth 8.7 cm from the front surface of the Li_2O assembly (located behind the FW/WCC and at a distance of 76.87 from the D-T neutron source). The Monte Carlo results were smeared using the NE213 windows. As shown, the spectrum between 2 - 10 MeV are larger in the calculations than those obtained by measurements NE213 results have large statistical errors below 2 MeV). This is shown in Fig. 5 where the calculated-to-experimental values (C/E) for the integrated spectrum in the energy range 2.05 <En <10.1 MeV are shown along the central axis. Along this axis, the C/E values obtained by the deterministic methods are very similar (C/E ~ 1.3 - 1.4) but the values obtained by the MORSE-DD/J3P1 (C/E ~ 1.4 - 1.1) and MCNP/RMCCS (C/E ~ 1.02 - 1.4) are different and have space-dependence. The statistical errors shown on the Monte Carlo results in this figure and in all subsequent figures are the combined calculational and experimental errors. These errors are large and are overlapping at most of the locations. The C/E for the integrated spectrum above 10.1 MeV is shown in Fig. 6 where the values are better than those shown in Fig. 5 (C/E ~ 0.9 - 1.1, except at deep locations with the Monte Carlo calculations). The DOT3.5 calculations (JAERI) give C/E values closer to unity and are lower than those obtained by the DOT 5.1/MATXS6 (U.S.) by ~ 10%. Notice that the 14 MeV peak is overestimated by DOT3.5 at front locations (See Fig. 4) although the integrated spectra above 10 MeV are lower than those obtained by the NE 213 measurements. Also, notice that the C/E values obtained by MORSE-DD calculations are lower than unity at all locations and also lower than the MCNP results. This is due to the lower spectrum above 10 MeV predicted by MORSE as compared to those obtained by MCNP as shown in Fig. 4.

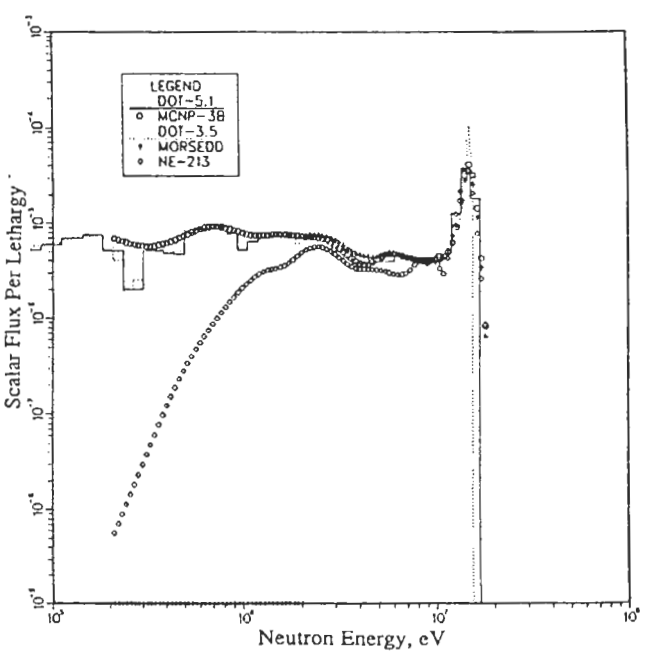

Figure 4. Measured and calculated neutron spectra at Z=8.7 cm (WCC experiment).

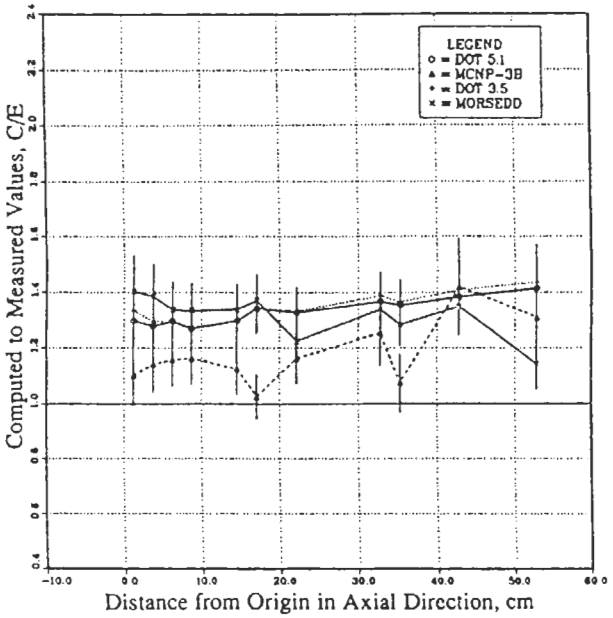

Figure 5. The C/E values for the interated spectrum, 2.05 MeV<En<10.1 MeV along the central axis (WCC experiment)

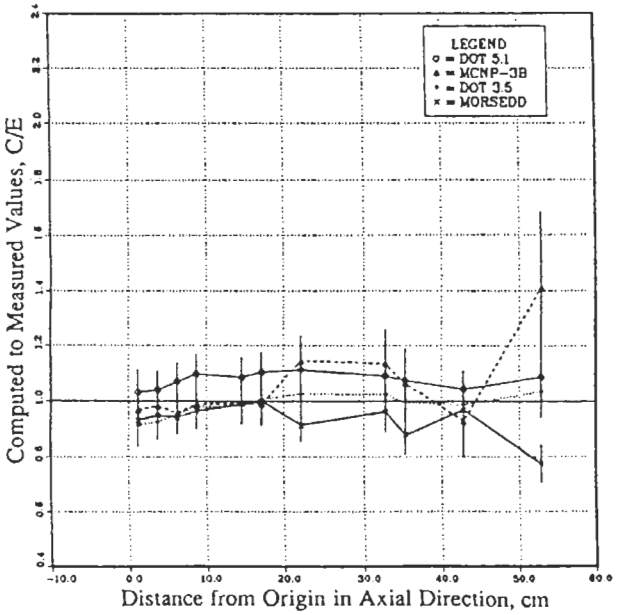

Figure 6. The C/E values for the integrated spectrum, En>10.1 MeV along the central axis (WCC experiment).

IV.A.2 Tritium Production and Other Reaction Rates

The C/E values for T_7 where measurements are performed by the NE213 indirect method are shown in Fig. 7. The value obtained by the U.S. (C/E ~ 1.1 - 1.25) are generally larger than those obtained by JAERI (C/E ~ 0.9 - 1.15) The feature of the curves shown relative to each other in the first 15 cm or so are similar to those shown in Fig. 6 but are shifted upward by ~ 10%. The similarity in the relative values is due to the fact that most of the contribution to T_7 at these front locations is due to neutrons above 10 MeV. The 10% shift could be due to the $^7Li(n,n'\alpha)t$ cross-section of JENDL3/PR1 used in folding the NE213 measured spectrum to estimate T_7. It was previously shown[3,6,8] from direct comparison between the JENDL3/PR1 cross-section for $^7Li(n,n'\alpha)t$ and Young's evaluation[27] used in the U.S. calculation that the former is lower than the latter by ~ 8 - 10%. Thus the experimental values obtained by NE213 method could be lower than what they should be which leads to the upward shift in the C/E values. This is supported by the fact that the T_7 measurements by the Li-foil technique are indeed lower than the NE213 measurements by ~ 10% throughout the test assembly and the C/E values in this case are closer to unity (not shown) than those shown in Fig. 7. The Li-foil technique requires long irradiation while the NE213 measurements are performed on-line.

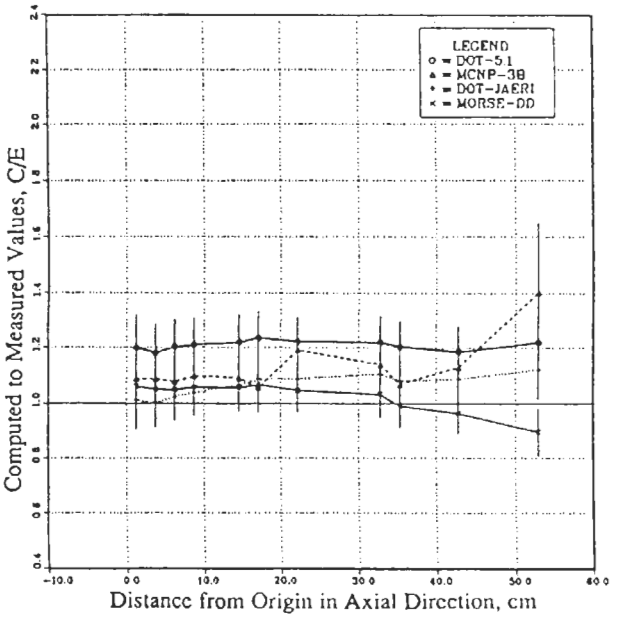

Figure 7. The C/E values for T_7 measured by NE213 detectors along the central axis (WCC experiment).

The C/E values for the high-threshold reaction $^{58}Ni(n, 2n)$ (E_{th} ~ 12.5 MeV) are shown in Fig. 8, where the U.S. values obtained by DOT 5.1 and MCNP are generally lower than unity by ~ 20 - 30% (except at few points in the middle of the test assembly in the MCNP calculations where the statistical errors are large). It was pointed out[3,6,8] that the $^{58}Ni(n,2n)$ cross-section as currently implemented in ENDF/B-V should be increased by ~ 25 - 30%. This would bring the C/E values closer to unity and to those obtained by JAERI.

The calculation for other high-threshold reactions are in general in good agreement with the measurements. The C/E for the $^{93}Nb(n, 2n)$ ^{92m}Nb (E_{th} ~ 8 MeV) are ~ 0.9 - 1.0 except at few locations toward the back of the assembly. The C/E values for $^{27}Al(n,\alpha)$ ^{24}Na (E_{th} ~ 6 Mev) are ~ 0.95

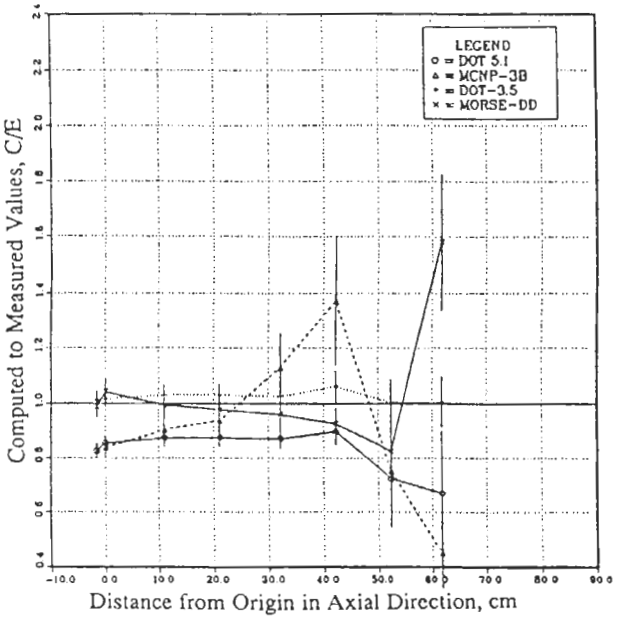

Figure 8. The C/E values for $^{58}Ni(n,2n)^{57}Ni$ reaction rate along the off-central axis (WCC experiment).

- 1.18 as predicted by all codes and data libraries while those for the $^{58}Ni(n,p)$ reaction (E_{th} ~ 2 MeV) are ranging from 1.1 - 1.3 at front locations to ~ 0.9 - 1.1 at the back locations (not shown). The overestimation could be partly attributed to the larger integrated spectrum in the energy range 2 - 10 MeV shown in Fig. 5. In the present work, it was shown in the U.S. analysis that the $^{58}Ni(n,p)$cross-section as currently implemented in the ACTL[30] library is underestimated by as much as 50% and should be revised in that activation library. For the $^{115}In(n, n')^{115m}In$ reaction, the agreement between calculations and measurements are very good (~ 5%) except in the MCNP calculations at the back locations. The prediction accuracies for the above threshold reactions by DOT 5.1/MATXS6 and DOT3.5/FSXJP7 are consistent among themselves while less consistency was observed between the NCNP/RMCCS and MORSE-DD/J3P1 results. The C/E values obtained by the latter tends to show a decreasing trend towards the back locations. As for non-threshold reactions such as ^{197}Au (n, γ) and ^{6}Li(n, α)t, the production profiles are very steep near the coolant channels. In addition the statistical errors in the Monte Carlo calculations are large. Fig. 9 shows the C/E values for the ^{197}Au(n, γ) reaction where noticeable change in the C/E values occurs near the coolant channel (depth of ~ 10 and 30 cm) and at the Li_2O/Li_2CO_3 boundaries. Around the coolant channels, the divergence between measurements and calculations are ~ 20 - 30%. This is also shown in Fig. 10 which depicts the C/E values for T_6 as measured by Li-glass detectors where the prediction accuracies are ± 20% (numerical values are given in Table II). With the Li-foil detectors, the C/E values for T_6 has improved. This can be seen from Fig. 11 where the calculations are those produced by DOT 5.1/MATXS 6. The improvement is in the range of 10-15%. In general, the prediction accuracy for threshold reactions were better than those for T_6 and ^{197}Au(n, γ) reactions. Nevertheless, it can be said that the prediction accuracies around heterogeneities are reasonable and that no essential difficulty is encountered in analyzing a heterogeneous system.

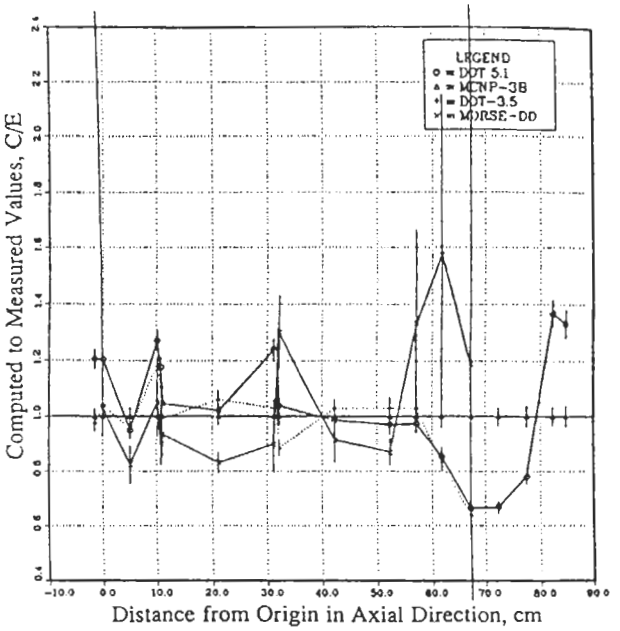

Figure 9. The C/E values for $^{197}Au(n,\gamma)^{198}Au$ reaction rate along the off-central axis (WCC experiment).

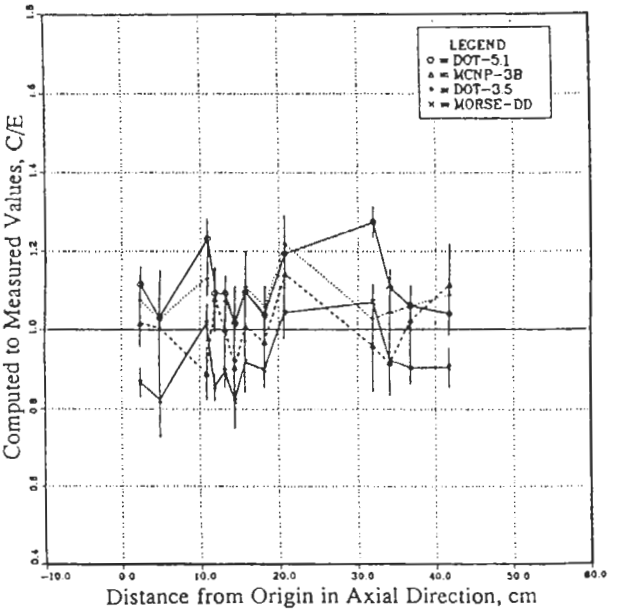

Figure 10. The C/E values for T_6 measured by Li-glass detectors along the central axis.

IV.B Beryllium Edge-On Experiment (BEO)

Arranging beryllium and Li_2O layers in an edge-on configuration resulted in a substantial increase in the local

TPR throughout the Li_2O layers. The pre-analysis indicated an increase of ~ 30% in the global tritium breeding ratio (TBR) in comparison to the case when no Be is introduced in the assembly. Local TPR from $^6Li(T_6)$ in the mixed zone (of depth 30 cm) increased by a factor of 3 in the central drawer as compared to the non-Be case (the reference experiment in phase IIA, see Refs. 3,6, and 8). This is due to the enhancement in the neutron population in the adjacent Be layers through Be(n,2n) reactions. T_7 also increased in the mixed region by ~ 8% but local values decreased thereafter by ~ 10% in comparison to the non-Be case.

The emerging neutrons from the Be Layers to the Li_2O layers have a noticeably large low-energy neutron component. Reactions that are sensitive to this component exhibit a depression at the center of the Li_2O layers with gradual increase towards the Be/Li_2 boundaries. Flux mapping of the low-energy neutrons was performed by $^{197}Au(n,\gamma)$ foil activation measurements in the vertical direction at the front face of the assembly and at a depth of 10 cm. The reaction rates get larger inside the Be layers and drop inside the Li_2O layers as one traverses these layers from bottom to top. The C/E values for this reaction at a depth of 10 cm are shown in Fig. 12 where the calculations were performed by MORSE-DD /J3P1 (JAERI). A large deviation can be observed in the order of ± 40% in the central layers while a deviation by a factor of 1.6 - 2.6 can be observed in the upper and lower most Li_2O layers. The statistical errors in the Monte Carlo calculations (not shown) are large. The error bars shown in figure 12 are the experimental errors only.

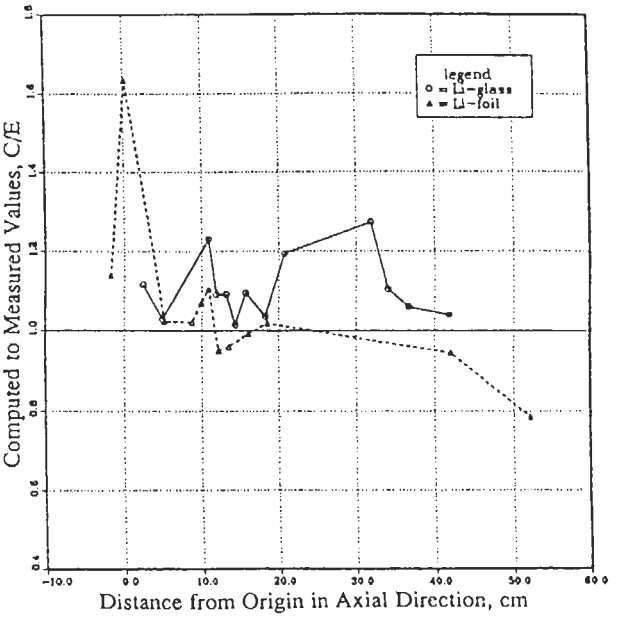

Figure 11. The C/E values for T6 measured by two detect types along the central axis (WCC Experiments).

Table II: Calculated-to-Experimental Values for T_6 Along the Central Axis in the Water Coolant Channel Experiment (Measurements by Li-glass detectors)

Position	Z(cm)*	Measured Value	Experimenal Error (%)	C/E Values					
				U.S.			JAERI		
				DOT 5.1	MCNP	S.E(%)+	DOT 3.5	MORSE-DD	S.E (%)+
1	2.40	1.107-28#	4.09	1.116	1.018	5.86	1.075	0.868	4.36
2	4.93	9.288-29	11.82	1.031	1.006	12.57	1.028	0.824	11.89
3	10.87	1.867-28	4.14	1.232	0.891	7.53	1.131	1.018	4.68
4	11.88	9.529-29	3.78	1.092	1.077	7.69	1.059	0.857	4.03
5	13.15	7.136-29	4.32	1.091	1.001	6.31	1.074	0.896	4.50
6	14.41	6.399-29	8.69	1.016	0.906	9.56	1.022	0.822	8.74
7	15.68	5.180-29	8.26	1.095	1.009	9.31	1.110	0.919	8.30
8	18.21	4.480-29	5.04	1.038	0.969	6.82	1.058	0.900	5.10
9	20.74	3.371-29	6.27	1.194	1.142	7.72	1.218	1.044	6.34
10	31.95	8.294-29	3.11	1.274	0.960	12.00	1.028	1.070	4.20
11	34.13	2.976-29	4.44	1.105	0.916	8.80	1.043	0.924	4.72
12	36.176	2.132-29	4.37	1.060	1.024	8.42	1.060	0.904	4.50
13	41.82	1.412-29	5.40	1.040	1.113	9.6	1.088	0.905	5.55

* Measured from the front edge of the Li_2O located behind the FW/PE layer. This edge is at a distance of 76.87 cm from D-T point source.

\# Reads 1.107×10^{-28} + $\sqrt{(\text{Experimental error})^2 + (\text{Monte Carlo Statistical error})^2}$

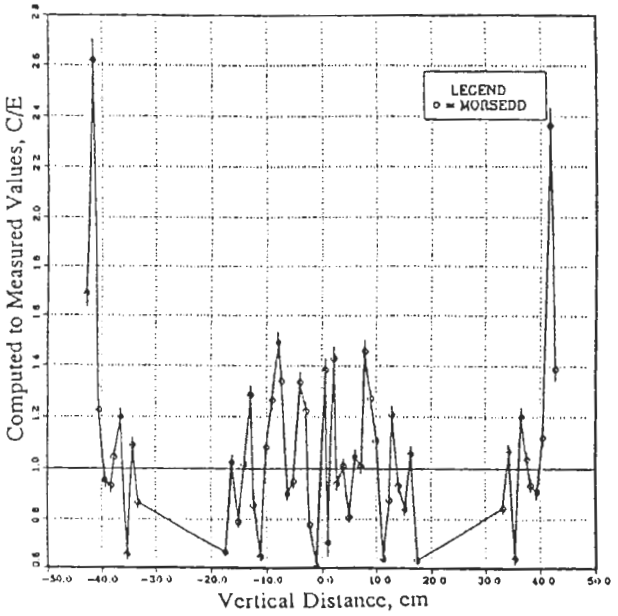

Figure 12. The C/E values for $^{197}Au(n,\gamma)\ ^{198}Au$ reaction rate in the vertical direction at a depth of 10 cm inside the test assembly (BOE experiment).

IV.B.1 In-System Spectrum Measurements

In-system spectrum measurements by NE213 were performed at depths of 1.2,6.2, 11.3, 21.5, 26.7, 31.6, 41.7, 51.8, and 72.1 cm along the axis of the central drawer. Fig. 13 shows a comparison between the calculated spectrum (by MCNP, U.S.) and the measured one at a depth of 11.3 cm (in the mixed zone) on the central axis. The agreement is reasonable in the energy range 2 - 10 MeV although the calculations show slightly larger values. The 14 MeV peak is underestimated and this is more noticeable as one proceeds toward the back locations. Figs. 14 and 15 show the C/E values for the integrated spectrum above 10.1 MeV and in the energy range 2.05 MeV<En<10.1 MeV, respectively as obtained by the U.S. and JAERI. The high energy component of the spectrum above 10.1 MeV is lower than the measured one by ~ 8-20% with large discrepancies occurring towards the back end of the assembly. On the other hand, the calculated spectrum in the energy range 2.05 MeV< En< 10.1 MeV is larger than the measurements by 40-5% with large discrepancies occurring at the front locations. These features are different from those shown in Figs. 5 and 6 in the WCC experiment and could be related to the beryllium data. It was discussed previously[8,10,28-29] that there are indications that the secondary neutron spectrum form the $^{9}Be(n,2n)$ reactions is overestimated in the energy range 2-10 MeV and underestimated above 10 MeV. Neutrons interacting inside the Be layers and emerging to the Li_2O layers have a spectrum that is underestimated above 10 MeV, as shown in Fig.14 while overestimation in the energy range 2-10 MeV is more pronounced at the front locations where more $^{9}Be(n,2n)$ reactions take place at the front of the mixed zone.

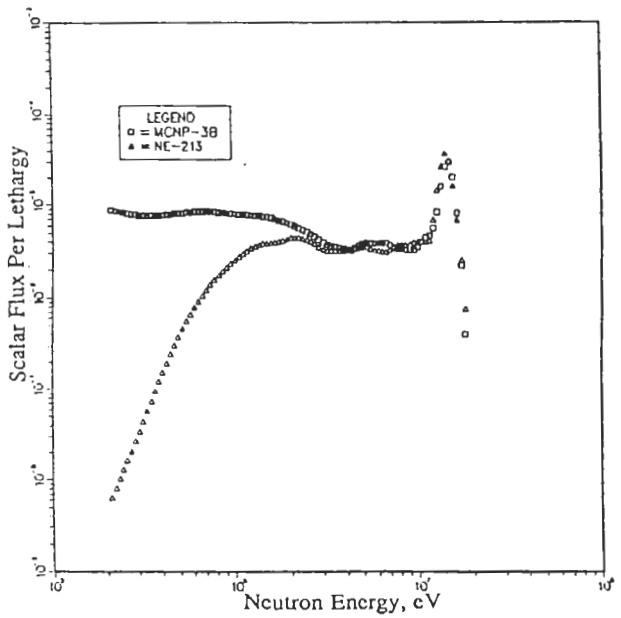

Figure 13. Measured and calculated neutron spectra (BEO experiment)

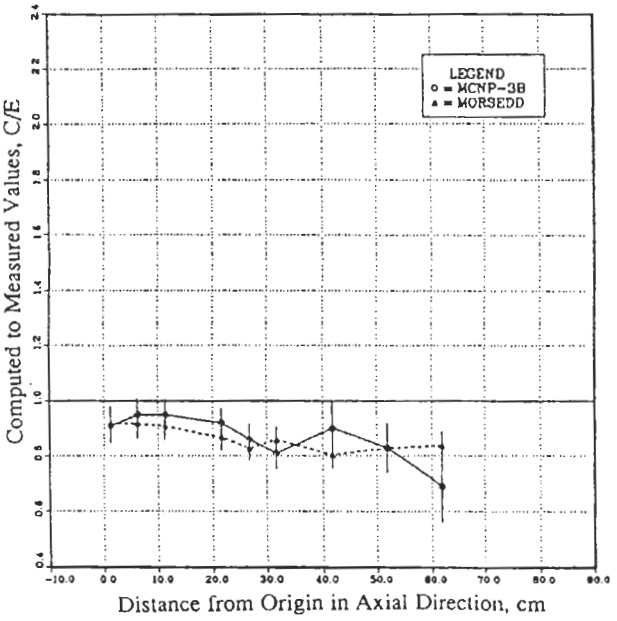

Figure 14. The C/E values for the integrated spectra, En>10.1 MeV along the central axis (BEO experiment).

IV.B.2 Tritium Production and Other Reaction Rates

The combination of the underestimation of the neutron spectrum above 10 MeV and overestimation in the energy range 2-10 MeV is reflected on the C/E values for T_7, as shown in Fig. 16. In comparison to the corresponding values in the WCC experiment, (See Fig. 7), the values shown in Fig. 16 have a decreasing trend as one moves to the back locations. The prediction accuracy in this case is within ± 10% and the U.S. values are on the average, larger than those obtained by JAERI by ~ 10% although there is an overlapping among the statistical errors in the Monte Carlo calculations at all locations.

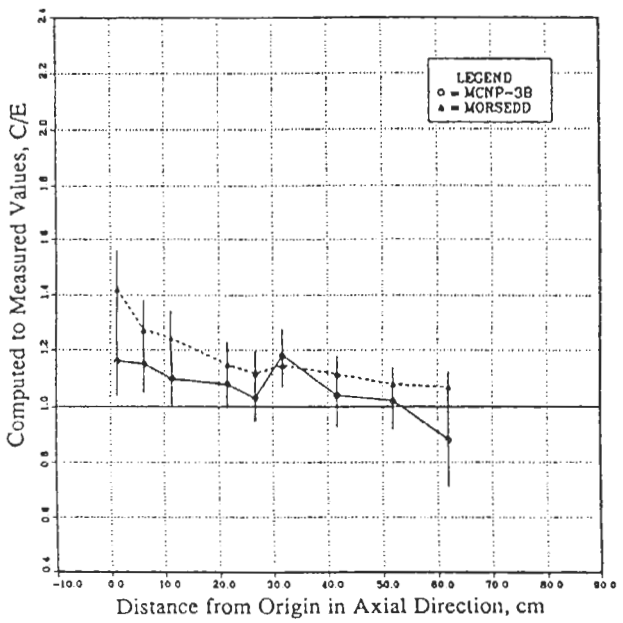

Figure 15. The C/E values for the integrated spectra 2.05MeV<En<10.1 MeV along the cenral axis (BEO experiment).

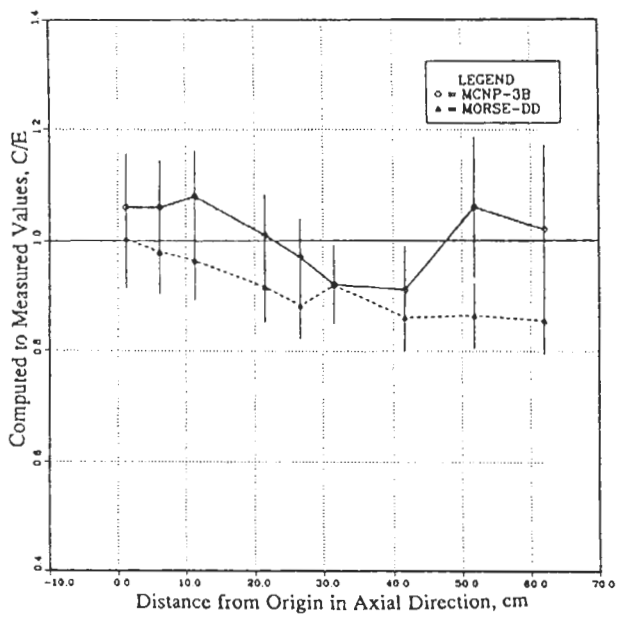

Figure 16. The C/E values for T_7 measured by NE213 detectors along the central axis (BEO experiment).

The prediction accuracies for other high-threshold reactions are reasonable. The $^{58}Ni(n,2n)$ and $^{93}Nb(n,2n)^{92m}Nb$ reactions have C/E values that are within ± 2% (as obtained by JAERI) at all locations along the central axis. Again, the U.S. calculations indicated a need to increase the $^{58}Ni(n,2n)$ cross-section of ENDF/B-V by 25-30% to yield better agreement with the experimental results. The $^{58}Ni(n,p)$ (E_{th} ~ 2 MeV) and $^{115}In(n,n')^{115m}In$ (E_{th} ~ 1 MeV) have C/E values that are within ± 7% and ± 10%, respectively. The C/E values for the $^{27}Al(n,\alpha)^{24}Na$ reactions (E_{th} ~ 6 MeV) are shown in Fig. 17 where they are also within ± 10%. It was noticed that the C/E curves for these threshold reactions tend to have a decreasing trend towards the back locations as does the C/E curve for the integrated spectrum above 10 MeV. The agreement among the U.S. and JAERI calculations and the measured values for $Ti(n,x)^{46}Sc$, and $Ti(n,x)^{47}Sc$) and $Ti(n,x)^{48}Sc$ is not as good as for other reactions and is basically due to differences in the cross-section values used by JAERI and the U.S.

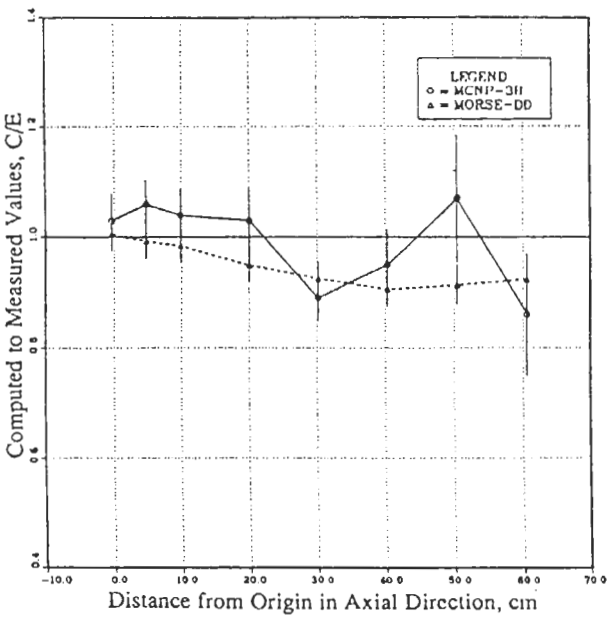

Figure 17. The C/E values for $^{27}Al(n,\alpha)^{24}Na$ reaction rate along the central axis (BEO experiment).

Fig. 18 shows the C/E values for $Ti(n,x)^{46}Sc$ where they are ~ 0.8 - 0.9 in the U.S. calculations while, on the average, are larger than unity (C/E ~ 1 -1.1) in JAERI's results. This reaction includes both the $^{47}Ti(n,np)^{46}Sc$ and the $^{46}Ti(n,p)^{46}Sc$ channels where the cross-sections are weighted by the natural abundance of ^{46}Ti and ^{47}Ti. Likewise, the C/E values for $Ti(n,x)^{47}Sc$ reactions are lower in the U.S. calculations by as much as 2-30% than those obtained by JAERI(C/E ~1.05) with a large divergence occurring at the front locations. On the other hand, the C/E values are larger in the U.S. Calculations for the $Ti(n,x)^{48}Sc$ reaction by ~ 10-40% than those obtained by JAERI(C/E ~ 1.02).

The C/E values for T_6 as measured by the Li-glass detectors are shown in Fig. 19. In comparison to Fig. 10, the values are more or less steady along the central axis with no abrupt changes in shape. The values obtained by the U.S. are generally larger (C/E ~ 0.8-1.05). In comparison to the no Be case (Reference case in phase IIA experiments, see Ref. 8), the C/E values are generally lower than unity by ~ 5-10% while in the no Be case the C/E values are generally larger than unity by ~ 7-10%. This could be again related to the beryllium data and/or to the flux perturbation caused by

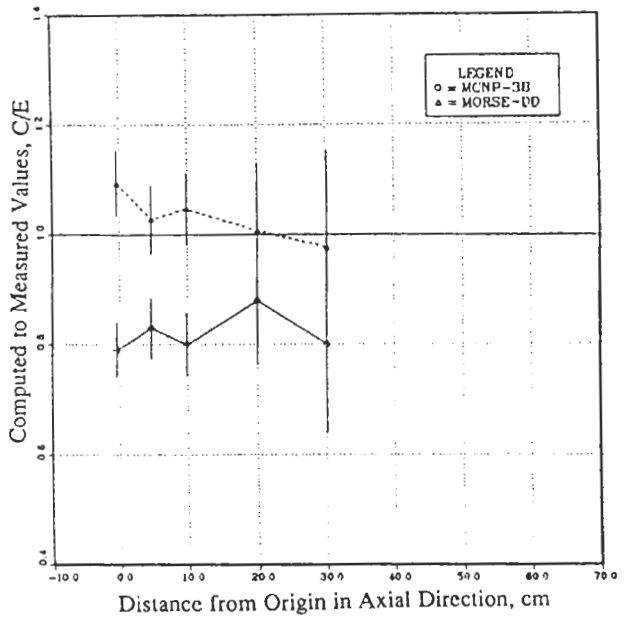

Figure 18. The C/E values for Ti(n,x)^{46}Sc reaction rate along the central axis (BEO experiment).

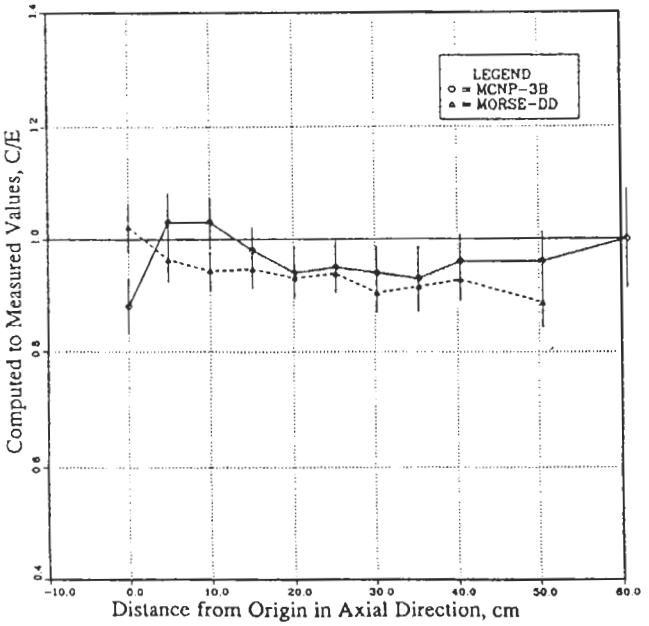

Figure 19. The C/E values for T_6 measured by Li-glass detectors along the central axis (BEO experiment).

the finite size of the Li-glass detectors used to measure T_6 in a softer spectrum as is the case in the BOE experiment.

As mentioned earlier, the TPR was also measured in predesignated zones along the central drawer (5.06 x 5.06 x 60 cm). Fig. 20 shows the C/E values from ^{N}Li(T_n) where the various axial distances for these zones can be inferred from Figure 20. The values are within ± 5% up to a depth of 45 cm. Thereafter, the C/E values are larger than unity by ~ 10-25% (the statistical errors in the back zones are as large as 20%). The C/E values for T_7 measured by this zonal technique are lower than unity in all zones by ~ 5-15% (not shown).

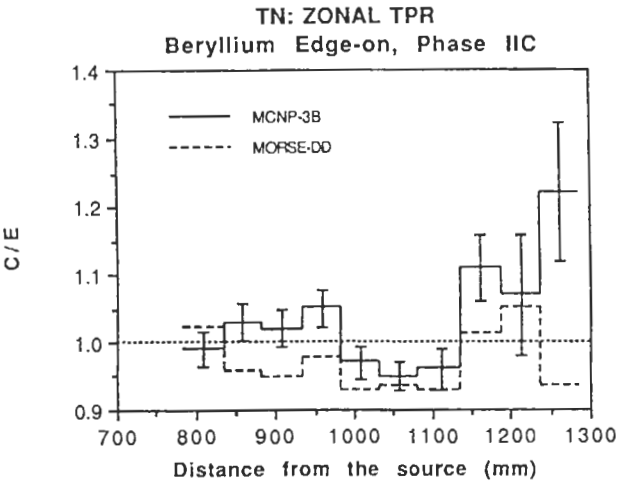

Figure 20. The C/E values for zonal T_n along the central drawer (BEO experiment).

V. SUMMARY

The coolant channels (WCC) and the beryllium edge-on (BEO) experiments were specifically chosen for Phase IIC in order to examine the prediction capabilities for tritium production, in-system spectra, and other reaction rates in systems that are characterized by design heterogeneities representative of various blanket designs. Comparisons were made to measurements and to results from previous phases of the experiments. In general, it was found that, even with system heterogeneities, the present codes and data libraries can reasonably predict the neutronics parameters with no specific difficulties. For high-threshold reactions (e.g.,^{58}Ni(n,2n), ^{93}Nb(n,2n)^{92m}Nb, etc.) the prediction accuracies are with ± 5-20% in the WCC system and within ± 10% in the BEO system. For these reactions, it was observed that there is a systematic difference between the Monte Carlo and the Sn method used to analyze the WCC system. In addition, the calculated-to-experimental (C/E) curves tend to decrease in the back region in both assemblies, particularly in the Monte Carlo calculations of the WCC system. For the threshold reactions, the results are consistent with previous phases (Phase IIA and IIB) although the C/E values tend to fall between the values obtained in these phases (C/E: IIB<IIC<IIA) up to a distance of ~ 30 cm. in the test assembly of the BEO system. The results show that the ^{58}Ni(n,2n) cross-section as currently implemented in ENDF/B-V (U.S.) should be increased by 25-30% to improve agreement with the experimental values. Also, the activation cross-section for ^{58}Ni(n,p) should be increased in the ACTL library (U.S.) by ~ 50%.

The prediction accuracy for T_7 in the WCC system were ± 15% in the JAERI calculations but a larger divergence was found in the U.S. calculations (C/E ~ 1.1-1.25) when the NE213 indirect method was used. Closer values to unity were observed in the BEO system (C/E ~ 0.9-1.1). The results obtained by the Li-foil measurements were better than those obtained by the NE213 method where improvement in the range of 10% is achieved. When zonal methods were applied to measure T_7, it was found that the C/E values are lower than unity by ~ 5-15% while TPR from natural lithium (T_N) is ± 5% up to a depth of 45 cm in the BEO system.

Unlike the threshold-reaction, the T_6 and $^{197}Au(n,\gamma)$ reactions exhibit steep profiles around the coolant channels in the WCC system while the $^{197}Au(n,\gamma)$ reaction shows large drops and increases as one vertically traverses the Be/Li_2O layers in the BEO system. The C/E curves for T_6 and $^{197}Au(n,\gamma)$ were not as flat as those for the high-threshold reactions when heterogeneities were crossed and gradients occured near them. The divergence in the calculations for T_6 around hetergeneities was about ± 20-25% (Li-glass detectors were used) and was ± 25-30% for $^{197}Au(n,\gamma)$ in the WCC system. With Li-foil detectors, the C/E values were improved by ~ 10-15%. In the BEO, the C/E values for T_6 were always less than unity where measurements were performed with Li-glass detectors. This could be related to the beryllium data since it was observed (as in the case in the other phases) that predictions were lower than measurements near Be/Li_2O boundaries. There are indications that the emission spectrum from the $^9Be(n,2n)$ reactions was underestimated below 0.5 MeV[8,10] and this could partly explain the lower values for the C/E curves for T_6 in the BOE system. The discrepancy could also be attributed to the geometrical effects of the Li-glass detector itself when used to measure T_6 in a soft spectrum. This study also showed that there are differences in the $Ti(n,x)^ySc(y=46,47,48)$ cross-sections between JENDL3 and ENDF/B-V evaluations that should be closely examined.

REFERENCES

(1) T. NAKAMURA and M. A. ABDOU, "Summary of Recent Results from the JAERI/U.S. Fusion Neutronics Phase I Experiments, Fusion Technol., 10, 541-548, 1986.

(2) M. Z. YOUSSEF, et al, "Analysis and Intercomparison for Phase I Fusion Integral Experiments at the FNS facility, Fusion Technol., 10, 549-563, 1986.

(3) M. Z. YOUSSEF, M. NAKAGAWA, et al, "Phase I Fusion Integral Experiments, Vol. II: Analysis," UCLA-ENG-88-15, University of California, Los Angeles, September, 1988. See also JAERI-M-88-177, Japan Atomic Energy Research Institute, Aug. 1988.

(4) M. NAKAGAWA et al, "Analysis of Neutronics Parameters Measured in Phase II Experiments of JAERI/U.S. Collaborative Program on Breeder Neutronics, Part I: Source Characteristics and Reaction Rate Distribution, Fusion Engr. and Design, 9, 315-322, 1989.

(5) Y. OYAMA et al, "Phase II Experimental Results of JAERI/USDOE Collaborative Program on Fusion Blanket Neutronics Experiments, Fusion Engr. and Design, 9, 309-313, 1989.

(6) M. Z. YOUSSEF et al, "Analysis of Neutronics Parameters Measured in Phase II Experiments of the JAERI/U.S. Collaborative Program on Fusion Blanket Neutronics, Part II: Tritium Production and In-System Spectrum, Fusion Engr. and Design, 9, 323-332, 1989.

(7) Y. OYAMA, et al, "Phase IIB Experiments of JAERI/USDOE Collaborative Program on Fusion Blanket Neutronics, Fusion Technol., 15 Number 2, Part 2B, 1293-1298, 1989.

(8) M. Z. YOUSSEF, et al, "Comparative Analysis for Phase IIA and IIB Experiments of the U.S./JAERI Collaborative Program on Fusion Breeder Neutronics", Fusion Technol., 15, 2, Part 2B, 1299-1308, 1989.

(9) Y. IKEDA, et al, "Determination of Neutron Spectrum in D-T Fusion Field by Foil Activation Technique, Fusion Technol., 15, 2, Part 2B, 1287-1292, 1989.

(10) M. Z. Youssef, et al, " The U.S./JAERI Collaborative Program on Fusion Neutronics; Phase IIA and IIB Fusion Integral Experiments, The U.S. Analysis: UCLA-ENG-90-14, University of California at Los Angeles, Dec. 1989.

(11) M. NAKAGAWA, et al., "JAERI/U.S. Collaborative Program on Fusion Blanket Neutronics, Analysis of Phase IIA and IIB Experiments, JAERI-M-89-154, Japan Atomic Energy Research Institute, October, 1989.

(12) Y. OYAMA, et al, "Measured Characteristics of Be Multi-layered and Coolant Channel Blankets: Phase IIC Experiments of the JAERI/USDOE Collaborative Program on Fusion Neutronics, this issue, 1990.

(13) A. KUMAR, et al, "Analysis of the Selection of Experimental Configuration For Heterogeneity and Be Multi-layered Experiments of the USDOE/JAERI Collaborative Program on Blanket Neutronics", Fusion Technol., 15, 2 Part 2b, 1309-1314, 1989.

(14) M. Z. YOUSSEF, et al, "Analysis for the Simulation of a line source by A 14 MeV moving point source and impact on blanket characteristics: The USDOE/JAERI Collaborative Program on Fusion Neutronics, this issue, 1990.

(15) T. NAKAMURA, et al, "A line D-T Neutron Source Facility for Annular Blanket Experiment: Phase III of the JAERI/USDOE Collaborative Program on Fusion Neutronics, this issue, 1990.

(16) Y. OYAMA, et al, "Annular Blanket Experiment Using A Line DT Neutron Source: Phase IIIA of the JAERI/USDOE Collaborative Program on Fusion Neutronics, this issue, 1990.

(17) C. KONNO, et al, "Measurements of the Source Term for Annular Blanket Experiment with A Line Source: Phase IIIA of the JAERI/USDOE Collaborative Program on Fusion Neutronics, this issue, 1990.

(18) A. KUMAR, et al, "Experiments and Analysis for Measurements of Decay Heat Related Induced Activities in Simulated Line Source Driven D-T Neutron Fields of Phase IIIA: JAERI/USDOE Collaborative Program on Fusion Neutronics, this issue, 1990.

(19) LOS ALAMOS MONTE CARLO GROUP, "MCNP--A General Monte Carlo Code for Neutron and Photon

Transport," version 3A, LA-7396, Rev. 2, Los Alamos National Laboratory, 1986.
(20) M. NAKAGAWA and T. MORI, "MORSE--DD, A Monte Carol Code Using Multigroup Double Differential Form Cross-Sections" JAERI-M84-126, Japan Atomic Energy Research Institute, July, 1984.
(21) R. MACFARLANE, "TRANSX-CTR: A Code for Interfacing MATXS Cross-Section Libraries to Nuclear Transport Codes for Fusion Systems Analysis," LA-9863-MS, Los Alamos National Laboratory, February, 1984.
(22) L. P. KU and J. KOLIBAL, "RUFF-A Ray Tracing Program to Generate Uncollided Flux and First Collision Source Moments for DOT4, A User's Manual, EAD-R-16, Plasma Physics Laboratory, Princeton University, 1980.
(23) W. A. RHOADES and R.L. CHILDS, "An Updated Version of the DOT 4 (version 4.3) One-and-Two-Dimensional Neutron/Photon Transport Code, ORNL-5851, Oak Ridge National Laboratory, (April, 1982). Also, see CCC-429, Radiation Shielding Information Center, RSIC, 1982.
(24) "DOT 3.5: Two-Dimensional Discrete Ordinates Radiation Transport Code, CCC-276, Radiation Shielding Information Center, RSIC," Also, see W.A. Rhoades and F.R. Mynett, "The DOT III Two-Dimensional Discrete Ordinates Transport Code," ORNL-TM-4280, Oak Ridge National Laboratory, September, 1973.
(25) R. A. MACFARLANE, "TRANSX-CTR: A Code for Interfacing MATXS Cross-Section, Libraries to Nuclear Transport Codes for Fusion Systems Analysis," LA-9863-MS, Los Alamos National Laboratory, February, 1984.
(26) J. BENVENISTE, et al., "The Problem of Measuring the Absolute Yield of 14-MeV Neutrons by Means of an Alpha counter," Nucl. Instrum. Method. 7, 306-314, 1960.
(27) P. G. YOUNG, "Evaluation of n+^{7}Li Reactions Using Variance-Covariance Techniques," Trans. Am Nucl. Soc., 39, 272, 1980.
(28) Y. OYAMA and H. MAEKAWA, "Measurements and Analysis of an Angular Neutron Flux on a Beryllium Slab Irradiated with Deuterium-Tritium Neutrons," Nucle. Sci. & Engr., 97, 220-234, 1987.
(29) M.Z. YOUSSEF and Y. WATANABE," Study on the Accuracy of Several Beryllium Data Evaluations and Comparison of Measured and Calculated data on Reaction Rates and Tritium Production Distributions, this issue, 1990.
(30) M. A. GARDNER and R. J. HOWERTON, "ACTL: Evaluated Neutron Activation Cross-Section Library _ Evaluation Techniques and Reaction Index," UCRL-50400, Vol. 18, Lawrence Livermore National Laboratory, October, 1978.